Taylor & Francis
Taylor & Francis Group

Optimization

A Journal of Mathematical Programming and Operations Research

ISSN: (Print) (Online) Journal homepage: https://www.tandfonline.com/loi/gopt20

Determination of the right-hand side in elliptic equations

Dinh Nho Hào, Le Thi Thu Giang & Nguyen Thi Ngoc Oanh

To cite this article: Dinh Nho Hào, Le Thi Thu Giang & Nguyen Thi Ngoc Oanh (2022): Determination of the right-hand side in elliptic equations, Optimization, DOI: 10.1080/02331934.2022.2141572

To link to this article: https://doi.org/10.1080/02331934.2022.2141572

Published online: 04 Nov 2022.

OPTIMIZATION
https://doi.org/10.1080/02331934.2022.2141572

Taylor & Francis
Taylor & Francis Group

Determination of the right-hand side in elliptic equations

Dinh Nho Hào[a], Le Thi Thu Giang[b] and Nguyen Thi Ngoc Oanh[c]

[a]Hanoi Institute of Mathematics, VAST, Hanoi, Vietnam; [b]Thuongmai University, Hanoi, Vietnam; [c]Thai Nguyen University of Sciences, Tan Thinh Ward, Thai Nguyen, Vietnam

ABSTRACT

The problem of determining a term in the right-hand side of elliptic equations from an observation on a part of the boundary is investigated. The inverse problem is formulated as an operator equation and then stabilized by Tikhonov regularization method. The regularized problem is discretized based on Hinze's variational discretization concept and the regularization parameter is chosen guaranteeing that when noise level and the discretization mesh size tend to zero, the solution of the discretized regularized problem converges to the f^*-minimum norm solution of the continuous inverse problem. Some numerical examples are presented for illustrating the performance of the proposed method.

ARTICLE HISTORY
Received 6 May 2022
Accepted 22 October 2022

KEYWORDS
Inverse source problem; elliptic equations; ill-posedness; regularization; finite element method

2010 MATHEMATICS SUBJECT CLASSIFICATIONS
35J15; 35R30; 65J20; 65N21

1. Introduction

The problem of determining sources in elliptic equations has attracted researchers for several decades, see e.g. [1–7]. Although there have been many papers dedicated to this inverse source problem, those with boundary observations are not many [1–17]. The existence, uniqueness and stability estimates for this inverse problem from boundary observations have been partially investigated in the above works. It appeared that the uniqueness is not guaranteed if the sought term in the right-hand side depends on all spatial variables. However, if this term is independent of one of the spatial variables, the uniqueness can be established, see. e.g. [7,17,18]. In this paper we consider a numerical method for solving the problem of reconstructing the right-hand side (source) $f(x)$ in the Robin problem for elliptic equations of the form:

$$\begin{cases} Lu = \hbar(x)f(x) + g(x), & x \in \Omega, \\ \dfrac{\partial u}{\partial \nu} + \sigma u = \varphi, & x \in \partial\Omega, \end{cases} \tag{1}$$

CONTACT Dinh Nho Hào hao@math.ac.vn

from the trace of the solution on a part Γ of the boundary $\partial\Omega$ (boundary observation):

$$u = \psi \quad \text{on } \Gamma. \tag{2}$$

Here, $\Omega \subset \mathbb{R}^n$ is a bounded domain with Lipschitz boundary $\partial\Omega$, the functions $\hbar, f, g \in L^2(\Omega), \varphi \in L^2(\partial\Omega)$ and $\psi \in L^2(\Gamma)$ are given, and L is an elliptic operator defined by

$$Lu = -\sum_{i,j=1}^{n} (a_{ij} u_{x_i})_{x_j} + au,$$

and

$$\frac{\partial u}{\partial \nu} = \sum_{i,j=1}^{n} (a_{ij} u_{x_i}) \nu_j,$$

where

$$\begin{gathered} a_{ij}, \quad a \in L^\infty(\Omega), \quad a \geq \bar{a} \geq 0, \quad \sigma \geq \bar{\sigma} \geq 0, \\ \sum_{i,j=1}^{n} a_{ij} \xi_i \xi_j \geq \lambda |\xi|^2_{\mathbb{R}^n}, \quad \forall \xi = (\xi_1, \ldots, \xi_n) \in \mathbb{R}^n, \\ \lambda \text{ isagivenpositiveconstant.} \end{gathered} \tag{3}$$

Since the inverse problem (1)–(2) may have many solutions, we introduce the so-called f^*-minimum norm solution which is nearest the a-priori f^* among all the solutions to it (Definition 2.3). In the next section we will show that the solution to the above inverse source problem is unstable. We then reformulate the problem in an abstract setting and study Tikhonov regularization for solving it. To solve the problem numerically we discretize the regularized problem by finite-dimensional problems based on Hinze's variational discretization concept in optimal control [19] to get error estimates. However, we go a little further than that for optimal control by Hinze, namely, we suggest a choice of the regularization parameter depending on the noise level in the observation data and the discretization mesh size which yields the convergence of the solution to the discretized regularized problem to the solution of the continuous inverse problem as these quantities tend to zero. This is one of the main contributions of this paper. Furthermore, with this choice a convergence rate is also established. In Section 3 we will apply this abstract result to the finite element method (FEM) for our inverse problem and finally in Section 4 some numerical examples are presented for illustrating the efficiency of our proposed method.

2. The inverse source problem and its abstract setting

2.1. The inverse problem as an operator equation

To deal with the inverse problem (1)–(2) we first introduce the notion of weak solutions to the direct problem (1).

Definition 2.1: A function $u \in H^1(\Omega)$ is called a weak solution to the boundary value problem (1) if the following equation holds for all $v \in H^1(\Omega)$:

$$\int_\Omega \sum_{i,j=1}^{n} a_{ij} u_{x_i} v_{x_j} \mathrm{d}x + \int_\Omega a u v \,\mathrm{d}x + \int_{\partial\Omega} \sigma u v \,\mathrm{d}s = \int_\Omega (\hbar f + g) v \,\mathrm{d}x + \int_{\partial\Omega} \varphi v \,\mathrm{d}s. \tag{4}$$

Denote

$$a[u,v] = \int_\Omega \sum_{i,j=1}^{n} a_{ij} u_{x_i} v_{x_j} \mathrm{d}x + \int_\Omega a u v \,\mathrm{d}x + \int_{\partial\Omega} \sigma u v \,\mathrm{d}s,$$

$$F(v) = \int_\Omega (\hbar f + g) v \,\mathrm{d}x + \int_{\partial\Omega} \varphi v \,\mathrm{d}s.$$

Then the weak solution $u \in H^1(\Omega)$ is defined as the solution to the variational equation

$$a[u,v] = F(v), \quad \forall\, v \in H^1(\Omega).$$

In the rest of this paper, if there is no more additional information required, we call *solution* instead of *weak solution* for brevity. It is well-known that (see [20, Theorem 2.7, p. 38], for instance):

Proposition 2.2: *If $\overline{a} + \overline{\sigma} > 0$, then for every $f, \hbar, g \in L^2(\Omega)$ and $\varphi \in L^2(\partial\Omega)$, problem (4) admits a unique solution $u \in H^1(\Omega)$. Moreover, there is some constant c_R, independent of $\hbar, f, g, \varphi$ such that*

$$\|u\|_{H^1(\Omega)} \le c_R \left(\|\hbar f\|_{L^2(\Omega)} + \|g\|_{L^2(\Omega)} + \|\varphi\|_{L^2(\partial\Omega)} \right). \tag{5}$$

We denote the solution to (1) by $u(x;f)$ (or $u(f)$ if there is no confusion) to emphasize the dependence of the solution u on f. The inverse source problem is to seek $f \in L^2(\Omega)$ such that (2) is satisfied.

Clearly, (1) can be splitted into the two following problems

$$L\bar{u} = \hbar(x)f(x), \quad x \in \Omega, \quad \frac{\partial \bar{u}}{\partial \nu} + \sigma \bar{u} = 0, \quad x \in \partial\Omega \tag{6}$$

and

$$L\tilde{u} = g(x), \quad x \in \Omega, \quad \frac{\partial \tilde{u}}{\partial \nu} + \sigma \tilde{u} = \varphi, \quad x \in \partial\Omega \tag{7}$$

for which

$$u = \bar{u} + \tilde{u}.$$

The solution $\tilde{u}$ of (7) is well-defined as all the data are given. The solution of the Robin problem (6) defines a linear bounded operator (the boundedness follows from (5)):

$$\begin{cases} A : L^2(\Omega) \to H^{\frac{1}{2}}(\Gamma) \hookrightarrow L^2(\Gamma) \\ \quad f \to Af = \bar{u}(f)|_\Gamma = (u - \tilde{u})|_\Gamma. \end{cases} \tag{8}$$

Since $H^{\frac{1}{2}}(\Gamma) \hookrightarrow L^2(\Gamma)$ is a compact embedding, A is a compact operator. Thus, the inverse source problem (1)–(2), which is equivalent to the operator equation

$$Af = \psi - \tilde{u}|_\Gamma := \tilde{\psi} \tag{9}$$

with the compact operator A, is ill-posed.

Now we give an example showing the ill-posedness of the inverse problem.

2.2. *Example on the instability.*

Let $\Omega = (0,1) \times (0,1)$, and $\alpha, \sigma_i, (i = 1,2,3,4)$ be known positive constants. Consider the problem of determining $f(x)$ in the system

$$\begin{cases} Lu := -\Delta u + \alpha u = f(x)\hbar(y), & (x,y) \in \Omega, \\ \dfrac{\partial u}{\partial x}(0,y) - \sigma_1 u(0,y) = 0, & y \in [0,1], \\ \dfrac{\partial u}{\partial x}(1,y) + \sigma_2 u(1,y) = 0, & y \in [0,1] \\ \dfrac{\partial u}{\partial y}(x,0) - \sigma_3 u(x,0) = 0, & x \in [0,1], \\ \dfrac{\partial u}{\partial y}(x,1) + \sigma_4 u(x,1) = 0, & x \in [0,1] \end{cases} \tag{10}$$

from the observation

$$u(x,0) = \psi(x), \quad x \in [0,1]. \tag{11}$$

The problem (10) can be solved by the method of separation of variables. In doing so, we consider the eigenvalue problem

$$\begin{cases} -\Delta u + \alpha u = \lambda u, & (x,y) \in \Omega, \\ \dfrac{\partial u}{\partial x}(0,y) - \sigma_1 u(0,y) = 0, & y \in [0,1], \\ \dfrac{\partial u}{\partial x}(1,y) + \sigma_2 u(1,y) = 0, & y \in [0,1], \\ \dfrac{\partial u}{\partial y}(x,0) - \sigma_3 u(x,0) = 0, & x \in [0,1], \\ \dfrac{\partial u}{\partial y}(x,1) + \sigma_4 u(x,1) = 0, & x \in [0,1]. \end{cases} \tag{12}$$

The eigenvalues and eigenfunctions $\lambda_{m,n}, u_{m,n}(x,y)$ are determined by the method of separation of variables. Following [21, p. 660], the eigenvalues have the form

$$\lambda_{m,n} = \mu_m^2 + \rho_n^2 + \alpha,$$

where μ_m and ρ_n are respectively the non-negative roots of the following equations

$$\tan \mu = \frac{(\sigma_1 + \sigma_2)\mu}{\mu^2 - \sigma_1\sigma_2}, \tag{13}$$

and

$$\tan \rho = \frac{(\sigma_3 + \sigma_4)\rho}{\rho^2 - \sigma_3\sigma_4}. \tag{14}$$

The corresponding eigenfunctions are

$$u_{m,n}(x,y) = \tilde{X}_m(x)\tilde{Y}_n(y),$$

where

$$\tilde{X}_m(x) = (\mu_m \cos \mu_m x + \sigma_1 \sin \mu_m x)\frac{1}{\sqrt{\mu_m^2 + \sigma_1^2}},$$

$$\tilde{Y}_n(y) = (\rho_n \cos \rho_n y + \sigma_3 \sin \rho_n y)\frac{1}{\sqrt{\rho_n^2 + \sigma_3^2}}.$$

For simplicity we suppose that $\sigma_1\sigma_2 = \sqrt{\pi/2}$. In Equation (13), on each interval $(-\pi/2 + 2m\pi, \pi/2 + 2m\pi), m = 0, 1, \ldots,$ the tangent function monotonically increases from $-\infty$ to ∞. Meanwhile, on the interval $[0, \sigma_1^2\sigma_2^2) = [0, \pi/2)$, the right-hand side of (13) monotonically decreases from zero to $-\infty$ and on $(\pi/2, \infty)$ it monotonically decreases from $+\infty$ to zero. Therefore, on each interval $(-\pi/2 + 2m\pi, \pi/2 + 2m\pi), m = 0, 1, \ldots,$ there always exists a unique root μ_n to (13), and $\mu_m \to +\infty$ as $m \to +\infty$. Similarly, if we suppose that $\sigma_3\sigma_4 =$

$\sqrt{\pi/2}$, then on each interval $(-\pi/2 + 2m\pi, \pi/2 + 2m\pi), m = 0, 1, \dots,$ there always exists a unique root ρ_m to (14), and $\rho_m \to +\infty$ as $m \to +\infty$. Set

$$X_m(x) = \frac{\tilde{X}_m(x)}{\|\tilde{X}_m\|_{L^2(0,1)}},$$
$$Y_m(y) = \frac{\tilde{Y}_n(y)}{\|\tilde{Y}_n\|_{L^2(0,1)}},$$
$$v_{m,n}(x,y) = \frac{u_{m,n}(x,y)}{\|u_{m,n}\|_{L^2(\Omega)}}.$$

Then $v_{m,n}(x,y), m, n = 0, 1, 2, \dots$ form an orthonormal basis system of the subspace consisting functions in $H^1(\Omega)$ which fulfill the boundary conditions in (10). Therefore, the solution to (10) has the form

$$u(x,y) = \sum_{m,n=0}^{\infty} c_{m,n} v_{m,n}(x,y), \tag{15}$$

where $c_{m,n}$ are constants to be determined. Substituting $u(x,y)$ into the first equation of (10) and noticing that $Lv_{mn} = \lambda_{mn} v_{mn}$, we have

$$\sum_{m,n=0}^{+\infty} \lambda_{mn} c_{mn} v_{mn}(x,y) = f(x)\hbar(y). \tag{16}$$

Multiplying the two sides of (15) by $v_{mn}(x,y)$ and integrating the product over Ω, we obtain

$$\lambda_{mn} c_{mn} = \langle f(x)\hbar(y), v_{mn}\rangle_{L^2(\Omega)} = \int_0^1 \int_0^1 f(x)\hbar(y) X_m(x) Y_n(y)\, \mathrm{d}x\, \mathrm{d}y = f_m \hbar_n.$$

Hence

$$c_{mn} = \frac{1}{\lambda_{mn}} f_m \hbar_n, \quad m, n = 0, 1, 2, \dots,$$

with $f_m = \langle f, X_m\rangle_{L^2(0,1)}$ and $\hbar_n = \langle \hbar, Y_n\rangle_{L^2(0,1)}$. Substituting c_{mn} into (11) and taking inner product the two sides by $\tilde{X}_m$, we have

$$\psi_m = \langle \psi; X_m\rangle_{L_2(\Omega)} = \sum_{n=1}^{+\infty} \frac{1}{\lambda_{mn}} f_m \hbar_n Y_n(0), \quad m = 0, 1, 2, \dots$$

where

$$\tilde{Y}_n(0) = \frac{\frac{\rho_n}{\sqrt{\rho_n^2 + \sigma_3^2}}}{\sqrt{\frac{1}{2} + \frac{(\sigma_1+\sigma_2)(\mu_m^2 + \sigma_1\sigma_2)}{(\mu_m^2+\sigma_1^2)(\mu_m^2+\sigma_2^2)}}} \leq \sqrt{2}.$$

Using the Cauchy–Schwarz inequality, with $m = 1, 2, \ldots,$ we have

$$
\begin{aligned}
|\psi_m|^2 &= |f_m|^2 \left(\sum_{n=0}^{+\infty} \frac{1}{\lambda_{mn}} |\hbar_n||Y_n(0)| \right)^2 \\
&\le 2|f_m|^2 \sum_{n=0}^{+\infty} \frac{1}{\lambda_{mn}^2} \sum_{n=1}^{+\infty} \hbar_n^2 = 2|f_m|^2 \sum_{n=1}^{+\infty} \frac{1}{(\mu_m^2 + \rho_n^2 + \alpha)^2} \|\hbar\|^2_{L^2(0,1)} \\
&\le 2|f_m|^2 \sum_{n=0}^{+\infty} \frac{1}{\lambda_{mn}^2} \sum_{n=0}^{+\infty} \hbar_n^2 = 2|f_m|^2 \sum_{n=0}^{+\infty} \frac{1}{4\mu_m^2 \rho_n^2} \|\hbar\|^2_{L^2(0,1)} \\
&= \frac{1}{2\mu_m^2} |f_m|^2 \|\hbar\|^2_{L^2(\Omega)} \sum_{n=0}^{+\infty} \frac{1}{\rho_n^2}.
\end{aligned}
$$

Here, we note that since $\mu_m \in (-\pi/2 + 2m\pi, \pi/2 + 2m\pi)$, the sum $\sum_{n=0}^{+\infty} \frac{1}{\rho_n^2}$ converges. It follows that

$$
|f_m| \ge \frac{\sqrt{2}\mu_m |\psi_m|}{\|\hbar\|_{L^2(0,1)} \sqrt{\sum_{n=0}^{+\infty} \frac{1}{\rho_n^2}}}. \tag{17}
$$

Since μ_m tends to $+\infty$ as m tends to $+\infty$, a small perturbation in ψ may cause a very large error in f_m which means that our inverse source problem is unstable.

2.3. The non-uniqueness of the solution

As said above, there are some examples showing the non-uniqueness of the inverse source problem [7,17,18] but not for the Robin problem. Now we present an example for this case. Let Ω be the rectangle $[a, b] \times [c, d]$. Suppose that (u_*, f_*) is a solution to problem (1)–(2). Then with an arbitrary function $T(x_1, x_2) \in H^1(\Omega)$, the pair $(u = u_* + \xi, f = f_* + \frac{L\xi}{\hbar})$, where $\xi = T(x_1, x_2)(x_1 - a)^2(x_1 - b)^2(x_2 - c)^2(x_2 - d)^2$, is also a solution to this problem. Similarly, if the term $f(x)$ depends only on x_1 but u is given on the x_2-axis, then the solution to the inverse problem is also not unique. For example, with $h(x) = 1, g(x) = 0$ and $f(x) = f(x_1)$ in problem (1), if (u_*, f_*) is a solution to the inverse source problem, then we can easily see that $(u = u_* + \xi_1, f = f_* + L\xi_1)$ is also a solution to it. Here $\xi_1 = (a - x_1)^2(b - x_1)^2 S(x_1)$ with $S(x_1)$ being an arbitrary function in $H^1[a, b]$.

2.4. Discretization of linear ill-posed problems

Let X be a Hilbert space with scalar product $\langle \cdot, \cdot \rangle_X$ and norm $\| \cdot \|_X$, Y be a Hilbert space with scalar product $\langle \cdot, \cdot \rangle_Y$ and norm $\| \cdot \|_Y$, and $A \in L(X, Y)$ be a compact linear operator. Consider the linear operator equation

$$Af = v. \tag{18}$$

This is an ill-posed problem, since A is compact.

Suppose that v is imprecisely given by v^ϵ:

$$\|v - v^\epsilon\|_Y \le \epsilon, \tag{19}$$

where $\epsilon > 0$ is the noise level.

As the problem (18) may have many solutions, we introduce the concept of f^*-minimum norm least squares solution to (18):

Definition 2.3: Let $f^* \in X$ be a priori given. The element $\hat{f} \in X$ is called f^*-minimum norm least squares solution (f^*-minimum norm solution for short) of problem (18) if

$$\|\hat{f} - f^*\|_X \le \|f - f^*\|_X$$

among those f minimizing the functional $\|Af - v\|_Y^2$.

It is standard to prove that if (18) has solutions, there exists a unique f^*-minimum norm solution to it. The problem of minimizing the functional $\|Af - v\|_Y^2$ itself is an ill-posed problem. So, in practice, $\hat{f}$ is approximated by $f_\alpha^\epsilon \in X$ which solves the regularized problem:

$$J_\alpha^\epsilon(f) = \frac{1}{2}\|Af - v^\epsilon\|_Y^2 + \frac{\alpha}{2}\|f - f^*\|_X^2 \to \min \tag{20}$$

with $\alpha > 0$ being the regularization parameter which has to be determined. It is proved that the problem (20) is well-posed and its unique solution f_α^ϵ satisfies the equation

$$J_\alpha^\epsilon(f)' = A^*(Af - v^\epsilon) + \alpha(f - f^*) = 0 \tag{21}$$

and f_α^ϵ is given by

$$f_\alpha^\epsilon = (A^*A + \alpha I)^{-1}(A^*v^\epsilon + \alpha f^*)$$

with A^* being the adjoint operator of A. Moreover, there are rules of choosing $\alpha = \alpha(\epsilon)$ such that when ϵ tends to 0, f_α^ϵ converges to $\hat{f}$. If certain source conditions are available, we have the rate of convergence as follows (see, e.g. [22, Theorem 2.12, p. 39]):

Assume that there exists a constant $\theta > 0$ and $w \in X$ such that

$$\|f^* - \hat{f}\|_X = (A^*A)^\theta w. \tag{22}$$

(a) Case 1: If $0 \le \theta \le 1$, then there exist positive constants C_1, C_2 such that

$$\|f_\alpha^\epsilon - \hat{f}\|_X \le \frac{C_1}{\sqrt{\alpha}}\epsilon + C_2\alpha^\theta. \tag{23}$$

(b) Case 2: If $\theta \geq 1$, then there exists a positive constant C_3 such that

$$\|f_\alpha^\epsilon - \hat{f}\|_X \leq C_1 \frac{\epsilon}{\sqrt{\alpha}} + C_3\alpha. \tag{24}$$

Remark 2.1: (a) To obtain an optimal convergence rate, we choose $\alpha = \mathcal{O}\epsilon^{\frac{2}{2\theta+1}}$, then f_α^ϵ converges to $\hat{f}$ with the rate of $\epsilon^{\frac{2\theta}{2\theta+1}}$ as ϵ tends to 0.

(b) In case $\theta = \frac{1}{2}$, $(A^*A)^{\frac{1}{2}}w = |A|w$, the convergence rate is $\epsilon^{\frac{1}{2}}$. Because the range of $(A^*A)^{\frac{1}{2}}$ and that of A^* are the same, there exists $w_1 \in Y$ such that $f^* - \hat{f} = |A|w_1 = A^*w_1$. Then

$$\|f_\alpha^0 - \hat{f}\| \leq \alpha(A^*A + \alpha I)^{-1}A^*w_1 \leq \frac{1}{2}\sqrt{\alpha}\|w_1\| = C_4\sqrt{\alpha}.$$

Hence,

$$\|f_\alpha^\epsilon - \hat{f}\| \leq C_1 \frac{\epsilon}{\sqrt{\alpha}} + C_4\sqrt{\alpha}.$$

Taking $\alpha = \mathcal{O}\epsilon$, we obtain that f_α^ϵ converges to $\hat{f}$ with the rate of $\epsilon^{\frac{1}{2}}$ which is the optimal rate in this particular case.

(c) In case $\theta \geq 1$, choosing $\alpha = \mathcal{O}\epsilon^{\frac{2}{3}}$ we get the optimal rate of $\epsilon^{\frac{2}{3}}$.

Now we will combine these results with Hinze's method [19] to get regularization parameters for the discretized regularized problem. In [19], Hinze has proven the following result.

Theorem 2.4: *Suppose that $Y_h \subset Y$ is a finite dimensional Hilbert subspace of Y, $A_h : X \to Y_h$ is a linear, bounded operator, $A_h^* : Y_h \to Y$ is the adjoint operator of A_h, f^+ and f_h^+ are respectively solutions to the problems*

$$\|Af - v\|_Y^2 + \alpha\|f - f^*\|_X^2 \to \min \tag{25}$$

and

$$\|A_h f - v\|_Y^2 + \alpha\|f - f^*\|_X^2 \to \min. \tag{26}$$

If

$$\begin{aligned} \|(A^* - A_h^*)v\|_X &\leq ch^2\|v\|_Y, \\ \|(A^*A - A_h^*A_h)f^+\|_X &\leq ch^2\|f^+\|_X, \end{aligned} \tag{27}$$

then

$$\|f^+ - f_h^+\|_X \leq c_1 h^2(\|f^+\|_X + \|v\|_Y). \tag{28}$$

with h being the mesh size of the discretization method.

The solution to (26) satisfies the optimality condition

$$A_h^*(A_hf - v) + \alpha(f - f^*) = 0. \tag{29}$$

Since A_h^* is a linear finite dimensional operator, it follows that, if $f^* \in X_h$, then $f_h^+ \in X_h$.

Remark 2.2: The result in the above theorem is still true if we substitute A_h by its approximation $\tilde{A}_h$ with $\|A_h - \tilde{A}_h\| < \delta < \frac{\alpha}{\|A_h\|}$.

Indeed, we have

$$A^*(Af^+ - v) + \alpha(f^+ - f^*) = 0, \tag{30}$$

$$\tilde{A}_h^*(A_hf_h^+ - v) + \alpha(f_h^+ - f^*) = 0. \tag{31}$$

Subtracting the second equation from the first one, we have

$$\alpha(f^+ - f_h^+) = -(A^*A - \tilde{A}_h^*A_h)f^+ - \tilde{A}_h^*A_h(f^+ - f_h^+) + (A^* - \tilde{A}_h^*)v. \tag{32}$$

Taking the inner product of both sides of (32) with $f^+ - f_h^+$, we have

$$\begin{aligned}
&\alpha\langle f^+ - f_h^+, f^+ - f_h^+\rangle_X \\
&\quad = -\langle (A^*A - \tilde{A}_h^*A_h)f^+, f^+ - f_h^+\rangle_X - \langle (\tilde{A}_h^* - A_h^*)A_h(f^+ - f_h^+), f^+ - f_h^+\rangle_X \\
&\qquad - \langle A_h^*A_h(f^+ - f_h^+), f^+ - f_h^+\rangle_X + \langle (A^* - \tilde{A}_h^*)v, f^+ - f_h^+\rangle_X \\
&\quad = -\langle (A^*A - \tilde{A}_h^*A_h)f^+, f^+ - f_h^+\rangle_X - \langle A_h(f^+ - f_h^+), (\tilde{A}_h - A_h)(f^+ - f_h^+)\rangle_X \\
&\qquad - \langle A_h(f^+ - f_h^+), A_h(f^+ - f_h^+)\rangle_Y + \langle (A^* - \tilde{A}_h^*)v, f^+ - f_h^+\rangle_X.
\end{aligned}$$

Since $\langle A_h(f^+ - f_h), A_h(f^+ - f_h)\rangle_Y = \|A_h(f^+ - f_h^+)\|_Y^2 \geq 0$, using Theorem 2.4 and the Cauchy–Schwarz inequality, we get

$$\begin{aligned}
\alpha\|f^+ - f_h^+\|_X^2 \leq{}& ch^2\|f^+\|_X\|f^+ - f_h^+\|_X + \|A_h\|\|\tilde{A}_h - A_h\|\|f^+ - f_h^+\|_X^2 \\
&+ ch^2\|v\|_Y\|f^+ - f_h^+\|_X \leq ch^2\|f^+\|_X\|f^+ - f_h^+\|_X + \delta\|A_h\|\|f^+ \\
&- f_h^+\|_X^2 + ch^2\|v\|_Y\|f^+ - f_h^+\|_X.
\end{aligned}$$

Hence,

$$(\alpha - \delta\|A_h\|)\|f^+ - f_h^+\|_X^2 \leq ch^2(\|f^+\|_X + \|v\|_Y)\|f^+ - f_h^+\|_X.$$

For $\delta < \frac{\alpha}{\|A_h\|}$, we have the inequality

$$\|f^+ - f_h^+\|_X \leq c_1h^2(\|f^+\|_X + \|v\|_Y), \tag{33}$$

with $c_1 = \frac{C}{\alpha - \delta\|A_h\|}$.

Remark 2.3: (1) If we replace assumptions (27) by

$$\begin{aligned} \|(A^* - A_h^*)v\|_X &\le Ch^{\beta_1}\|v\|_Y, \\ \|(A^*A - A_h^*A_h)f^+\|_X &\le Ch^{\beta_2}\|f^+\|_X, \end{aligned} \tag{34}$$

for $\beta_1, \beta_2 > 0$, then the estimate (28) has the form

$$\|f^+ - f_h^+\|_X \le Ch^{\beta}(\|f^+\|_X + \|v\|_Y), \quad \beta = \min\{\beta_1, \beta_2\}. \tag{35}$$

(2) Supposing similar assumptions:

$$\begin{aligned} \|(A^* - A_h^*)v\|_X &\le \mathcal{O}(h^{\beta_1}), \\ \|(A^*A - A_h^*A_h)f^+\| &\le \mathcal{O}(h^{\beta_2}), \end{aligned} \tag{36}$$

we have

$$\|f^+ - f_h^+\|_X \le \mathcal{O}(h^{\beta}), \quad \beta = \min\{\beta_1, \beta_2\}. \tag{37}$$

The following theorem provides rules for choosing a priori regularization parameters depending on the mesh size h and error level ϵ which guarantees that the solution to the discretized regularized problem converges to the f^*-minimum norm least squares solution of the continuous inverse problem. Furthermore, if the source condition (22) is satisfied, then the rate of convergence can be obtained.

Theorem 2.5: *Let X, Y be Hilbert spaces, and A be a compact operator in $L(X, Y)$. Suppose that $Y_h \subset Y$ is a finite dimensional subspace, $A_h : X \to Y_h$ is a linear, bounded operator and $A_h^* : Y_h \to X$ is the adjoint operator of A_h. Furthermore, suppose that A and A_h satisfy the assumption (34). Let $f_{\alpha h}^{\epsilon}$ be the solution of the variational problem*

$$\|A_h f - v^{\epsilon}\|_Y^2 + \alpha\|f - f^*\|_X^2 \to \min. \tag{38}$$

Assume that the source condition (22) is satisfied. Then the following statements hold.

(a) *If $0 \le \theta \le 1$ and $\alpha = \mathcal{O}(\epsilon^{\frac{2}{2\theta+1}} + h^{\frac{\beta}{\theta+1}})$, then $f_{\alpha h}^{\epsilon}$ converges to the f^*-minimum norm solution of problem (18) in X-norm with the convergence rate $\mathcal{O}(\epsilon^{\frac{2\theta}{2\theta+1}} + h^{\frac{\beta\theta}{\theta+1}})$.*
(b) *If $\theta \ge 1$ and $\alpha = \mathcal{O}(\epsilon^{\frac{2}{3}} + h^{\frac{\beta}{2}})$, then $f_{\alpha h}^{\epsilon}$ converges to the f^*-minimum norm solution of problem (18) with the convergence rate $\mathcal{O}(\epsilon^{\frac{2}{3}} + h^{\frac{\beta}{2}})$.*

Proof: We have

$$\|f^{\epsilon}_{\alpha h} - \hat{f}\|_X \le \|f^{\epsilon}_{\alpha h} - f^{\epsilon}_{\alpha}\|_X + \|f^{\epsilon}_{\alpha} - \hat{f}\|_X, \tag{39}$$

where f^{ϵ}_{α} and $f^{\epsilon}_{\alpha h}$ are the solutions of

$$A^*(Af_\alpha - v^\epsilon) + \alpha(f_\alpha - f^*) = 0 \quad \text{and}$$
$$A^*_h(A_h f_{\alpha h} - v^\epsilon) + \alpha(f_{\alpha h} - f^*) = 0,$$

, respectively. From these equations, we obtain

$$\alpha(f^{\epsilon}_{\alpha} - f^{\epsilon}_{\alpha h}) = A^*_h A_h(f^{\epsilon}_{\alpha h} - f^{\epsilon}_{\alpha}) + (A^*_h A_h - A^*A)f^{\epsilon}_{\alpha} + (A^* - A^*_h)v^\epsilon. \tag{40}$$

Taking the inner product both sides of (40) with $f^{\epsilon}_{\alpha} - f^{\epsilon}_{\alpha h}$, we get

$$\begin{aligned}
&\alpha\|f^{\epsilon}_{\alpha} - f^{\epsilon}_{\alpha h}\|^2_X \\
&\quad = -\langle A^*_h A_h(f^{\epsilon}_{\alpha h} - f^{\epsilon}_{\alpha}), f^{\epsilon}_{\alpha h} - f^{\epsilon}_{\alpha}\rangle_X \\
&\qquad - \langle (A^*A - A^*_h A_h)f^{\epsilon}_{\alpha}, f^{\epsilon}_{\alpha} - f^{\epsilon}_{\alpha h}\rangle_X + \langle (A^* - A^*_h)v^\epsilon, f^{\epsilon}_{\alpha} - f^{\epsilon}_{\alpha h}\rangle_X \\
&\quad = -\|A_h(f^{\epsilon}_{\alpha}) - f^{\epsilon}_{\alpha h})\|^2_X - \langle (A^*A - A^*_h A_h)f^{\epsilon}_{\alpha}, f^{\epsilon}_{\alpha} - f^{\epsilon}_{\alpha h}\rangle_X \\
&\qquad + \langle (A^* - A^*_h)v^\epsilon, f^{\epsilon}_{\alpha} - f^{\epsilon}_{\alpha h}\rangle_X \le \|(A^*A - A^*_h A_h)f^{\epsilon}_{\alpha}\|_X\|f^{\epsilon}_{\alpha} - f^{\epsilon}_{\alpha h}\|_X \\
&\qquad + \|(A^* - A^*_h)v^\epsilon\|_X\|f^{\epsilon}_{\alpha} - f^{\epsilon}_{\alpha h}\|_X.
\end{aligned}$$

Hence

$$\begin{aligned}
\|f^{\epsilon}_{\alpha} - f^{\epsilon}_{\alpha h}\|_X &\le \frac{1}{\alpha}\left(\|(A^*A - A^*_h A_h)f^{\epsilon}_{\alpha}\|_X + \|(A^* - A^*_h)v^\epsilon\|_X\right) \\
&\le \frac{1}{\alpha}(Ch^\beta\|f^{\epsilon}_{\alpha}\|_X + Ch^\beta\|v^\epsilon\|_Y) = \frac{Bh^\beta}{\alpha},
\end{aligned}$$

If the source condition (22) is satisfied, using estimates (23) and (24), we have

(a) If $0 \le \theta \le 1$:

$$\|f^{\epsilon}_{\alpha h} - \hat{f}\|_X \le \frac{C_1\epsilon}{\sqrt{\alpha}} + C_2\alpha^\theta + \frac{Bh^\beta}{\alpha}.$$

Clearly, with $\alpha = \mathcal{O}(\epsilon^{\frac{2}{2\theta+1}} + h^{\frac{\beta}{\theta+1}})$, we have

$$\|f^{\epsilon}_{\alpha h} - \hat{f}\|_X \le \mathcal{O}\left(\epsilon^{\frac{2\theta}{2\theta+1}} + h^{\frac{\beta\theta}{\theta+1}}\right).$$

(b) If $\theta \ge 1$, then

$$\|f^{\epsilon}_{\alpha h} - \hat{f}\|_X \le \frac{C_1\epsilon}{\sqrt{\alpha}} + C_2\alpha + \frac{Bh^\beta}{\alpha}.$$

In this case, with $\alpha = \mathcal{O}(\epsilon^{\frac{2}{3}} + h^{\frac{\beta}{2}})$, we have

$$\|f^{\epsilon}_{\alpha h} - \hat{f}\|_X \le \mathcal{O}\left(\epsilon^{\frac{2}{3}} + h^{\frac{\beta}{2}}\right).$$

In the next section we will applied these results to the inverse problem of determining f in (1)–(2). ■

3. The inverse source problem and its finite element approximation

3.1. The inverse problem

In the previous section, we showed that the problem of determining the right-hand side f in (1)–(2) can be rewritten as the operator equation (9). Suppose that ψ is imprecisely given by ψ^ϵ such that

$$\|\psi - \psi^\epsilon\|_{L^2(\Gamma)} \leq \epsilon. \tag{41}$$

Suppose that f^* is an a priori prediction for f. Then following the above section, the regularized problem for determining f from the noisy data ψ^ϵ has the form

$$\begin{aligned}\min_{f\in L_2(\Omega)} J_\alpha(f) &= \min_{f\in L^2(\Omega)} \left\{\frac{1}{2}\|u(f)|_\Gamma - \psi^\epsilon\|^2_{L_2(\Gamma)} + \frac{\alpha}{2}\|f - f^*\|^2_{L^2(\Omega)}\right\} \\ &:= \min_{f\in L^2(\Omega)} \left\{\frac{1}{2}\|Af - \tilde{\psi}^\epsilon\|^2_{L^2(\Gamma)} + \frac{\alpha}{2}\|f - f^*\|^2_{L^2(\Omega)}\right\}.\end{aligned} \tag{42}$$

Here, A is defined by (8), $\tilde{\psi}^\epsilon = \psi^\epsilon - \tilde{u}|_\Gamma$, $\alpha > 0$ is the Tikhonov regularization parameter.

By the standard scheme, it can be proved that (42) has a unique solution, the functional J_α is Fréchet differentiable and its derivative has the form

$$J'_\alpha(f) = A^*(Af - \tilde{\psi}^\epsilon) + \alpha(f - f^*). \tag{43}$$

Here $A^* : L_2(\Gamma) \to L_2(\Omega)$ is the adjoint operator of A. To define $A^*(Af - \tilde{\psi}^\epsilon) = A^*(u(f) - \psi^\epsilon)$, we consider the adjoint problem to (6):

$$\begin{cases} Lp = 0, & x \in \Omega, \\ \dfrac{\partial p}{\partial \nu} + \sigma p = \begin{cases} \Phi(x), & x \in \Gamma, \\ 0, & x \in \partial\Omega \setminus \Gamma. \end{cases} \end{cases} \tag{44}$$

Lemma 3.1: *The adjoint operator $A^* : L^2(\Gamma) \to L^2(\Omega)$ of A is defined by*

$$A^*\Phi = \hbar p,$$

where $p = p(x)$ is the solution to the adjoint problem (44).

Proof: Since p is the solution to (44), for all $\xi \in H^1(\Omega)$, we have

$$\int_\Omega \sum_{i,j=1}^n a_{ij} p_{x_i} \xi_{x_j} \mathrm{d}x + \int_\Omega a(x) p \xi(x)\,\mathrm{d}x + \int_{\partial\Omega} \sigma(x) p \xi(x)\,\mathrm{d}s = \int_\Gamma \phi(x)\xi(x)\,\mathrm{d}s. \tag{45}$$

Similarly, $\bar{u} = \bar{u}(x)$ is the solution of (6) if following equality satisfies for all $v \in H^1(\Omega)$

$$\int_\Omega \sum_{i,j=1}^n a_{ij} \bar{u}_{x_i} v_{x_j} \mathrm{d}x + \int_\Omega a\bar{u}v\,\mathrm{d}x + \int_{\partial\Omega} \sigma\bar{u}v\,\mathrm{d}s = \int_\Omega \hbar(x) f(x) v(x)\,\mathrm{d}x. \tag{46}$$

Substituting $\xi(x)$ in (45) by the solution $\bar{u}(x)$ of (46) and $v(x)$ in (46) by the solution $p(x)$ of (45), we have

$$\int_\Omega \hbar(x)f(x)p(x)\,\mathrm{d}x = \int_\Gamma \Phi(x)\bar{u}(x)\,\mathrm{d}s = \int_\Gamma \Phi(x)Af\,\mathrm{d}s.$$

Hence,

$$\langle \hbar p, f\rangle_{L^2(\Omega)} = \langle Af, \Phi(x)\rangle_{L^2(\Gamma)} = \langle A^*\Phi(x), f\rangle_{L^2(\Omega)}.$$

The above result indicates that

$$A^*\Phi(x) = \hbar(x)p(x)$$

with $p(x)$ is the solution to Equation (44). ■

We summarize these results in the following theorem.

Theorem 3.2: *The functional $J_\alpha(f)$ is Fréchet differential and its derivative has the form*

$$J'_\alpha(f) = \hbar(x)p(x) + \alpha(f - f^*),$$

where $p(x)$ is the solution to the adjoint system

$$\begin{cases} Lp = 0, \quad x \in \Omega, \\ \dfrac{\partial p}{\partial \nu} + \sigma p = \begin{cases} u(f) - \psi^\epsilon(x), & x \in \Gamma, \\ 0, & x \in \partial\Omega \setminus \Gamma. \end{cases} \end{cases} \tag{47}$$

The solution to the variational problem (42) is the solution to the equation $J'_\alpha(f) = 0$.

Remark 3.1: In this case, the source conditions can be represented as follow:

(1) **The first source condition:** There exists $\Phi \in L^2(\partial\Omega)$ such that $f - f^* = \hbar(x)p(x)$ in which p is the solution of problem (44).
(2) **The second source condition**: There exists $\phi \in L^2(\Omega)$ such that $f - f^* = A^*A\phi$. Similarly, we can state this condition by the existence of $\phi \in L^2(\Omega)$ such that $f - f^* = \hbar p$, with p being the solution of the problem:

$$\begin{cases} Lp = 0, \quad x \in \Omega, \\ \dfrac{\partial p}{\partial \nu} + \sigma p = \begin{cases} \bar{v}(x), & x \in \Gamma, \\ 0, & x \in \partial\Omega \setminus \Gamma. \end{cases} \end{cases} \tag{48}$$

Here, $\bar{v}(x) = v(x)|_\Gamma$, with $v(x)$ being the solution of the problem

$$\begin{cases} Lv = \hbar(x)\phi(x), & x \in \Omega, \\ \dfrac{\partial v}{\partial \nu} + \sigma v = 0, & x \in \partial\Omega. \end{cases} \tag{49}$$

3.2. Conjugate gradient method

In this part, we will present the conjugate gradient method for solving the minimization problem (42). Assume that f^k is an approximate of f at the kth iteration, then the next one is

$$f^{k+1} = f^k + \nu^k d^k,$$

where

$$d^k = \begin{cases} -\nabla J_\alpha(f^k) & \text{if } k = 0, \\ -\nabla J_\alpha(f^k) + \gamma^k d^{k-1} & \text{if } k > 0, \end{cases} \tag{50}$$

and

$$\gamma^k = \frac{\|\nabla J_\alpha(f^k)\|^2_{L^2(\Omega)}}{\|\nabla J_\alpha(f^{k-1})\|^2_{L^2(\Omega)}} \quad \text{and} \quad \nu^k = \text{argmin}_{\nu>0} J_\alpha(f^k + \nu d^k). \tag{51}$$

To evaluate ν^k, let us rewrite $J_\alpha(f^k + \nu d^k)$ as follows:

$$\begin{aligned} J_\alpha(f^k + \nu d^k) &= \frac{1}{2}\|u(f^k + \nu d^k)|_\Gamma - \psi^\epsilon\|^2_{L^2(\Gamma)} + \frac{\alpha}{2}\|f^k + \nu d^k - f^*\|^2_{L^2(\Omega)} \\ &= \frac{1}{2}\|A(f^k + \nu d^k) - (\psi^\epsilon - \tilde{u}|_\Gamma)\|^2_{L^2(\Gamma)} + \frac{\alpha}{2}\|f^k + \nu d^k - f^*\|^2_{L^2(\Omega)} \\ &= \frac{1}{2}\|\nu A d^k + A f^k - (\psi^\epsilon - \tilde{u}|_\Gamma)\|^2_{L^2(\Gamma)} + \frac{\alpha}{2}\|\nu d^k + f^k - f^*\|^2_{L^2(\Omega)}. \end{aligned}$$

Differentiating of $J_\alpha(f^{k+1})$ respect to ν, we get

$$\begin{aligned} \frac{\partial J_\alpha(f^k + \nu d^k)}{\partial \nu} &= \|Ad^k\|^2_{L^2(\Omega)}\nu + \langle Ad^k, Af^k - (\psi^\epsilon - \tilde{u}|_\Gamma)\rangle_{L^2(\Gamma)} \\ &+ \alpha\|d^k\|^2_{L^2(\Omega)}\nu + \alpha\langle d^k, f^k - f^\star\rangle_{L^2(\Omega)} \end{aligned}$$

Letting

$$\frac{\partial J_\alpha(f^k + \nu d^k)}{\partial \nu} = 0,$$

we have

$$\nu^k = -\frac{\langle d^k, \nabla J_\alpha(f^k)\rangle_{L^2(\Omega)}}{\|Ad^k\|^2_{L^2(\Gamma)} + \alpha\|d^k\|^2_{L^2(\Omega)}}.$$

The CG method is summarized as follows

(1) *Step 1:*
   (a) Initiate f^0.
   (b) Solve the direct problem to compute $u(f^0)$

$$\begin{cases} Lu = \hbar f^0 + g, & x \in \Omega, \\ \dfrac{\partial u}{\partial \nu} + \sigma u = \varphi, & x \in \partial\Omega. \end{cases}$$

(c) Calculate $\nabla J_\alpha(f^0) = \hbar p^0$, where p^0 solves the adjoint problem

$$\begin{cases} Lp = 0, \quad x \in \Omega, \\ \dfrac{\partial p}{\partial \nu} + \sigma p = \begin{cases} u(f^0) - \psi^\epsilon, & x \in \Gamma, \\ 0, & x \in \partial\Omega \setminus \Gamma. \end{cases} \end{cases}$$

(d) Calculate

$$d^0 = -\nabla J_\alpha(f^0), \quad \nu^0 = \frac{\|\nabla J_\alpha(f^0)\|^2_{L^2(\Omega)}}{\|Ad^0\|^2_{L^2(\Gamma)} + \alpha\|d^0\|^2_{L^2(\Omega)}}.$$

Update

$$f^1 = f^0 + \nu^0 d^0.$$

(2) *Step 2:* For $k = 1, 2, \ldots$

(a) Solve the direct problem to calculate $u(f^k)$

$$\begin{cases} Lu = \hbar f^k + g, & x \in \Omega, \\ \dfrac{\partial u}{\partial \nu} + \sigma u = \varphi, & x \in \partial\Omega. \end{cases}$$

(b) Calculate $\nabla J_\alpha(f^k) = \hbar p^k$, where p^k solves the adjoint problem

$$\begin{cases} Lp = 0, \quad x \in \Omega, \\ \dfrac{\partial p}{\partial \nu} + \sigma p = \begin{cases} u(f^k)|_\Gamma - \psi^\epsilon, & x \in \Gamma, \\ 0, & x \in \partial\Omega \setminus \Gamma. \end{cases} \end{cases}$$

(c) Calculate

$$\gamma^k = \frac{\|\nabla J_\alpha(f^k)\|^2_{L^2(\Omega)}}{\|\nabla J_\alpha(f^{k-1})\|^2_{L^2(\Omega)}}, \quad d^k = -\nabla J_\alpha(f^k) + \gamma^k d^{k-1},$$

(d) Solve the direct problem

$$\begin{cases} Lv^k = \hbar d^k, & x \in \Omega, \\ \dfrac{\partial v^k}{\partial \nu} + \sigma v^k = 0, & x \in \partial\Omega. \end{cases}$$

(e) Calculate

$$Ad^k = v^k|_\Gamma, \quad \nu^k = \frac{\|\nabla J_\alpha(f^k)\|^2_{L^2(\Omega)}}{\|Ad^k\|^2_{L^2(\Gamma)} + \alpha\|d^k\|^2_{L^2(\Omega)}}.$$

(3) *Step 3*: Update

$$f^{k+1} = f^k + \nu^k d^k.$$

To apply this scheme we need to solve the direct and adjoint problems. For this purpose, we use the finite element method (FEM).

3.3. Finite element method for the direct problem

We use spaces of piecewise polynomial functions as approximation spaces X_h of $X \subset L^2(\Omega)$. Suppose that the bounded domain $\Omega \subset \mathbb{R}^n, n = 1, 2, 3,$ is divided into subdivisions $T_h = \{K\}$. For $n = 1$, the elements K are intervals, for $n = 2$ they are triangles or quadrilaterals and for $n = 3$ they are tetrahedrons for instance. The approximation space X_h is assumed to satisfy $X_h \subset H^1(\Omega)$. This condition is equivalent to $X_h \subset C^0(\bar{\Omega})$, where $C^0(\bar{\Omega}) = \{v : v \mathrm{isacontinuousfunctiondefinedon} \bar{\Omega}\}$.

We first consider the case $X = H^1(\Omega)$ and $X_h = \{v \in V : v|_K \in P_1(K), \forall K \in T_h\}$, where $T_h = \{K\}$ is a triangulation of $\Omega \subset \mathbb{R}^2$, i.e. X_h is the standard finite element space of piecewise linear functions on triangles K. For $K \in T_h$ we call h_K the longest side of K, d_K is the diameter of the circle inscribed in K and $h = \max_{K \in T_h}\{h_K\}$. We further require that there is a positive constant β independent of $K \in T_h$ such that $\frac{d_K}{h_K} \geq \beta, \ \forall K \in T_h$.

Definition 3.3: A function $u_h = u_h(x) \in X_h$ is called an FE (finite element) solution to the boundary problem (1) in X_h if for all $v_h = v_h(x) \in X_h$, the following equality holds

$$\int_\Omega \sum_{i,j=1}^{N} a_{ij} u_{h_{x_i}} v_{h_{x_j}} \mathrm{d}x + \int_\Omega a u_h v_h \mathrm{d}x + \int_{\partial\Omega} \sigma u_h v_h \mathrm{d}s = \int_\Omega (\hbar(x) f(x) + g(x)) v_h \mathrm{d}x + \int_{\partial\Omega} \varphi(x) v_h \mathrm{d}s. \tag{52}$$

Denote by

$$a[u_h, v_h] = \int_\Omega \left(\sum_{i,j=1}^{n} a_{ij}(x) u_{h_{x_i}} v_{h_{x_j}} + a(x) u_h(x) v_h(x) \right) \times \mathrm{d}x + \int_{\partial\Omega} \sigma(x) u_h(x) v_h(x) \, \mathrm{d}s(x),$$

$$F(v_h) = \int_\Omega \left((f(x)\hbar(x) + g(x) \right) v_h(x) \, \mathrm{d}x + \int_{\partial\Omega} \varphi(x) v_h \, \mathrm{d}s(x),$$

$$k = 1, 2, \ldots N.$$

Then u_h is the solution to Equation (52) if the following variational equation holds

$$a[u_h, v_h] = F(v_h)$$

for all $v_h \in X_h$. Let $\{\varphi_1, \varphi_2, \ldots, \varphi_N\}$ be a basis for X_h. Then u_h has the unique representation

$$u_h = \sum_{l=1}^{N} \xi_l \varphi_l, \quad \xi_l \in \mathbb{R}, \tag{53}$$

which leads to the system

$$\sum_{l=1}^{N} a[\varphi_k, \varphi_l]\xi_l = F(\varphi_k), \quad k = 1, 2, \ldots, N. \tag{54}$$

Denoting

$$\begin{aligned} &A = (A_{lk})_{N\times N}, \quad \text{with } A_{lk} = a[\varphi_l, \varphi_k], B = (B_k)_{N\times 1} \quad \text{with} \\ &B_k = F(\varphi_k) \quad \text{and} \quad \Xi = (\xi_l)_{N\times 1}. \end{aligned}$$

(54) can be represented by

$$A\Xi = B. \tag{55}$$

It is standard to prove that A is positive definite and therefore (55) is uniquely solvable.

Theorem 3.4 ([23, p. 91]): *If Ω is an open, bounded domain in $\mathbb{R}^n$, u and u_h are respectively the weak solution and the FE solution to Equation (1), then there is a constant C independent on u and h such that*

$$\|u - u_h\|_{L^2(\Omega)} \le Ch\|u\|_{H^1(\Omega)}. \tag{56}$$

The FE solution to (6) denoted by $\bar{u}_h$ defines a linear operator

$$\begin{aligned} A_h :& L^2(\Omega) \to L^2(\Gamma), \\ & f \mapsto A_h(f) = \bar{u}_h(f)|_\Gamma. \end{aligned}$$

We see that A_h is an approximation of A and its adjoint A_h^* approximates A^*.

Proposition 3.5: *The adjoint operator to A_h is defined by*

$$\begin{aligned} A_h^* :& L^2(\Gamma) \to L^2(\Omega), \\ & \phi \mapsto A_h^*\phi = \hbar(x)p_h(x), \end{aligned}$$

with $p_h(x)$ being the FE solution of (44).

Proof: The proof of this assertion is similar to that of Theorem 3.1.

Since p_h is the FE solution of (44), for all $\xi(x) \in X_h$, we have

$$\int_\Omega \sum_{i,j=1}^n a_{ij} p_{hx_i} \xi_{x_j} \mathrm{d}x + \int_\Omega a(x) p_h \xi(x) \,\mathrm{d}x + \int_{\partial\Omega} \sigma(x) p_h \xi(x) \,\mathrm{d}s = \int_\Gamma \phi(x)\xi(x) \,\mathrm{d}s. \tag{57}$$

Similarly, $\bar{u}_h = \bar{u}_h(x)$ is the solution of (6) if following equality is satisfied for all $v = v(x) \in X_h(\Omega)$

$$\int_\Omega \sum_{i,j=1}^n a_{ij} \bar{u}_{hx_i} v_{x_j} \mathrm{d}x + \int_\Omega a\bar{u}_h v \,\mathrm{d}x + \int_{\partial\Omega} \sigma \bar{u}_h v \,\mathrm{d}s = \int_\Omega \hbar(x) f(x) v(x) \,\mathrm{d}x. \tag{58}$$

Substituting $\xi(x)$ in (57) by the solution $\bar{u}_h(x)$ of (58) and $v(x)$ in (46) by the solution $p_h(x)$ of (57), we have

$$\int_\Omega h(x) f(x) p_h(x) \,\mathrm{d}x = \int_\Gamma \Phi(x) \bar{u}_h(x) \,\mathrm{d}s = \int_\Gamma \Phi(x) A_h f \,\mathrm{d}s.$$

Hence,

$$\langle \hbar p_h, f\rangle_{L^2(\Omega)} = \langle A_h f, \Phi(x)\rangle_{L^2(\Gamma)} = \langle A_h^* \Phi(x), f\rangle_{L^2(\Omega)}.$$

The above result indicates that

$$A_h^* \Phi(x) = \hbar(x) p_h(x)$$

with $p_h(x)$ being the solution to Equation (44). ∎

We now prove that A, A^*, A_h and A_h^* satisfy Assumptions (27).

Proposition 3.6: *With A, A^*, A_h, A_h^* being operators defined above, for every $y \in L^2(\Gamma)$ and $f \in L^2(\Omega)$, there exist constants C_1 independent of y, h and C_2 independent of f, h such that*

$$\begin{aligned} \|(A^* - A_h^*)y\|_{L^2(\Omega)} &\le C_1 h \|y\|_{L^2(\Gamma)}, \\ \|(A^*A - A_h^* A_h)f\|_{L^2(\Omega)} &\le C_2 h \|f\|_{L^2(\Omega)}. \end{aligned} \tag{59}$$

Proof: Indeed, recall that for $y \in L^2(\Gamma)$, $A^* y = h(x)p(x)$ and $A_h^* y = h(x) p_h(x)$, where $p(x)$ and $p_h(x)$ are the exact solution and FE solution to the problem:

$$\begin{cases} Lp = 0, \\ \dfrac{\partial p}{\partial \nu} + \sigma p = \begin{cases} y, & x \in \Gamma, \\ 0, & x \in \partial\Omega \setminus \Gamma. \end{cases} \end{cases}$$

Therefore,

$$\|(A^* - A_h^*)y\|_{L^2(\Omega)} = \|\hbar(p - p_h)\|_{L^2(\Omega)} \le \|\hbar\|_{L^2(\Omega)} \|p - p_h\|_{L^2(\Omega)}.$$

Since $\hbar(\cdot) \in L^2(\Omega)$, it follows from the estimate (5) that there is a constant C_1 which depends only on $\hbar(x), f(x)$ and the coefficients of Equation (1) such that

$$\|(A^* - A_h^*)y\|_{L^2(\Omega)} \le C_1 h \|y\|_{L^2(\Gamma)}. \tag{60}$$

For all $f \in L^2(\Omega)$, we have

$$\|(A^*A - A_h^*A_h)f\|_{L^2(\Omega)} \le \|A^*(A - A_h)f\|_{L^2(\Omega)} + \|(A^* - A_h^*)A_h f\|_{L^2(\Omega)}.$$

The second term is easy to evaluate as we can directly apply (60):

$$\|(A^* - A_h^*)A_h f\|_{L^2(\Omega)} \le C_1 h \|A_h f\|_{L^2(\Gamma)} \le C_1 h \|A_h\| \|f\|_{L^2(\Omega)}. \tag{61}$$

To estimate the first term, we notice that $Af = \bar{u}(f)|_\Gamma$ and $A_h f = \bar{u}_h(f)|_\Gamma$ with $\bar{u}$ and $\bar{u}_h$ being the weak solution and FE solution, respectively, to the problem

$$\begin{cases} L\bar{u} = \hbar(x)f(x), \\ \dfrac{\partial \bar{u}}{\partial \nu} + \sigma \bar{u} = 0, \quad x \in \partial\Omega, \end{cases}$$

and $A_h f$ is its FE approximation or $A_h f = \bar{u}_h|_\Gamma$. Hence

$$\|(A - A_h)f\|_{L^2(\Gamma)} = \|(\bar{u} - \bar{u}_h)(f)\|_{L^2(\Gamma)} \le \|\bar{u} - \bar{u}_h\| \|f\|_{L^2(\Omega)} \le Ch\|f\|_{L^2(\Omega)}.$$

Furthermore, $A^*(A - A_h)f = \hbar(x)p(x)$ in which $p(x)$ solves the following problem

$$\begin{cases} Lp = 0, \\ \dfrac{\partial p}{\partial \nu} + \sigma p = \begin{cases} (A - A_h)f, & x \in \Gamma, \\ 0, & x \in \partial\Omega \setminus \Gamma. \end{cases} \end{cases}$$

Therefore,

$$\begin{aligned} \|A^*(A - A_h)f\|_{L^2(\Omega)} &\le \|\hbar\|_{L^2(\Omega)} \|p\|_{L^2(\Omega)} \le \|\hbar\|_{L^2(\Omega)} \|(A - A_h)f\|_{L^2(\Gamma)} \\ &\le C_2 h \|f\|_{L^2(\Omega)}. \end{aligned} \tag{62}$$

From the estimates (61) and (62), the assertion follows. ■

If the right-hand side and the boundary conditions of (1) are more regular, then is so u.

Proposition 3.7 ([24, Corollary 2.2.2.4, p. 91, Corollary 2.2.2.6, p. 92 and Theorem 2.3.3.6, p. 110)]): *Let Ω be a bounded open set with a $C^{1,1}$ boundary, $A = (a_{ij})$ is Lipschitz in $\bar{\Omega}$. If σ is Lipschitz in $\bar{\Omega}$, $\varphi \in H^{\frac{1}{2}}(\partial\Omega)$, then there exists a unique weak solution u to (1) in $H^2(\Omega)$ such that*

$$\|u\|_{H^2(\Omega)} \le C\left(\|\hbar f\|_{L^2(\Omega)} + \|g\|_{L^2(\Omega)} + \|\varphi\|_{H^{\frac{1}{2}}(\partial\Omega)}\right). \tag{63}$$

Under the conditions of the above proposition, we can get a better error estimate of the FEM for (1). Precisely, there exists a constant C independent of h, u, such that [23, p. 91]

$$\|u - u_h\|_{L^2(\Omega)} \leq Ch^2\|u\|_{H^2(\Omega)} \leq Ch^2\|u\|_{H^2(\Omega)}.$$

Applying Proposition 3.7, we can prove that in this case, Hinze's assumptions are fulfilled as follows:

Proposition 3.8: *With A, A^*, A_h, A_h^* being operators defined above, for every $v \in H^{\frac{1}{2}}(\Gamma)$ and $f \in L^2(\Omega)$, there exist constants C_1 independent on v, h and C_2 independent on f, h such that*

$$\begin{aligned} \|(A^* - A_h^*)v\|_{L^2(\Omega)} &\leq C_1 h^2 \|v\|_{H^{\frac{1}{2}}(\Gamma)}, \\ \|(A^*A - A_h^*A_h)f\|_{L^2(\Omega)} &\leq C_2 h^2 \|f\|_{L^2(\Omega)}. \end{aligned} \tag{64}$$

The proof of this proposition is similar to that of Proposition 3.6.

3.4. Regularized discretized variational problem

The discretized version of the optimization problem (42) has the form

$$\min_{f\in L^2(\Omega)} J_\alpha^h(f) = \min_{f\in L^2(\Omega)} \left\{ \frac{1}{2}\|u^h(f)|_\Gamma - \psi^\epsilon\|^2_{L^2(\Gamma)} + \frac{\alpha}{2}\|f - f^*\|^2_{L^2(\Omega)} \right\}. \tag{65}$$

This problem has a unique solution $f_{h,\alpha}^\epsilon$. Furthermore, based on the above analysis, we can conclude that $f_{h,\alpha}^\epsilon$ satisfies the optimality condition

$$\begin{aligned} &u_h = u_h(x) := u_h(f) \in X_h, \\ &\quad \int_\Omega \sum_{i,j=1}^N a_{ij} u_{h_{x_i}} v_{h_{x_j}} \mathrm{d}x + \int_\Omega a u_h v_h \mathrm{d}x + \int_{\partial\Omega} \sigma u_h v_h \mathrm{d}s \\ &\qquad = \int_\Omega (\hbar(x) f(x) + g(x)) v_h \mathrm{d}x + \int_{\partial\Omega} \varphi v_h \mathrm{d}s, \quad \text{forall } v_h = v_h(x) \in X_h, \end{aligned} \tag{66}$$

$$\begin{aligned} &p_h = p_h(x) \in X_h, \\ &\quad \int_\Omega \sum_{i,j=1}^N a_{ij} p_{hx_i} \xi_{x_j} \mathrm{d}x + \int_\Omega a(x) p_h \xi(x)\, \mathrm{d}x + \int_{\partial\Omega} \sigma p_h \xi\, \mathrm{d}s \\ &\qquad = \int_\Gamma (u_h(f) - \psi^\epsilon) \xi\, \mathrm{d}s, \quad \text{forall } \xi \in X_h, \end{aligned} \tag{67}$$

$$\hbar(x) p_h(x) + \alpha(f - f^*) = 0. \tag{68}$$

The regularization parameter α is now chosen according to Theorem 2.5 that guarantees the convergence of $f^{\epsilon}_{h,\alpha}$ to f^{+} of the inverse source problem (1)–(2) as ϵ and h tend to zero.

4. Numerical examples

In this section we present some numerical examples for two cases: that with uniqueness and that without uniqueness. We test these examples for observations on the whole boundary or on a part of it, and for the sought-for term of different smoothness. We note that it is very difficult to verify the source condition (22), therefore we first test our examples without knowing it. Next, we will provide some examples in which the source condition is satisfied in some approximate sense.

Consider problem (1)–(2) with $\Omega = (0,1)\times(0,1) \subset \mathbb{R}^2, \Gamma_1 := (0,1)\times\{0\}$, $\Gamma_2 := \{0\}\times(0,1), \Gamma_3 := (0,1)\times\{1\}, \Gamma_4 := \{1\}\times(0,1), \partial\Omega = \bar{\Gamma}_1 \cup \bar{\Gamma}_2 \cup \bar{\Gamma}_3 \cup \bar{\Gamma}_4$ and $Lu = -\sum_{i,j=1}^{2}(a_{ij}u_{x_i})_{x_j} + au$ with

$$\begin{cases} a_{11} = x_1 + x_2^2 + 1, \quad a_{12} = a_{21} = x_1x_2, \quad a_{22} = x_2^2 + 2, \\ a(x) = 1 + x_1 + x_2. \end{cases} \tag{69}$$

We prescribe $u = x_1 \sin \pi x_2 + x_1 + 2x_2^2 - 1, \sigma(x) = x_1^2 + x_2 + 1$, and $\hbar(x) = 1$. Then, on the boundary $\partial\Omega$ we have the boundary condition $\frac{\partial u}{\partial \nu} + \sigma u = \varphi$ with

$$\varphi(x) = \begin{cases} -2\pi x_1 + (x_1^2+1)(x_1-1), & x_2 \in \Gamma_1, \\ (x_2^2+2)(\sin \pi x_2 + 1) + x_2(\pi \cos(\pi x_2) + 4x_2) & \\ \quad +(x_2+2)(\sin \pi x_2 + 2x_2^2), & x \in \Gamma_2, \\ x_1 + 3(-\pi x_1 + 4) + (x_1^2+2)(x_1+1), & x \in \Gamma_3, \\ -(x_2^2+1)(\sin(\pi x_2)+1) + (x_2+1)(2x_2^2-1), & x \in \Gamma_4. \end{cases} \tag{70}$$

Since u is given, we have

$$\begin{aligned} Lu(x) = &- \sin \pi x_2 - x_2(\pi x_1 \cos \pi x_2 + 4x_2) - \pi x_1 x_2 \cos \pi x_2 - x_1(\sin \pi x_2 + 1) \\ &- 2x_2(\pi \cos \pi x_2 + 4x_2) \\ &+ (x_2^2+2)(\pi^2 x_1 \sin \pi x_2 - 4) + (1 + x_1 + x_2) \\ &\times (x_1 \sin \pi x_2 + x_1 + 2x_2^2 - 1) - 1. \end{aligned}$$

Thus, $Lu(x) = f(x) + g(x)$. For numerical experiments, we choose f and thus have $g(x) = Lu(x) - f(x)$, and try to reconstruct it from an observation of u on a part of the boundary of Ω.

For the finite element discretization we use a uniform triangulation of the domain Ω into 65536 elements.

Table 1. Example 4.1: L_2-error in the smooth case.

Relative noise (%)	0.1	1	0.1	1	0.1
Observation	$\Gamma_1 \cup \Gamma_2$	$\Gamma_1 \cup \Gamma_2$	Γ	Γ	$\Gamma_2 \cup \Gamma_4$
L_2-error	0.0778591	0.0844967	0.042706	0.0579043	0.172632

Example 4.1 (The solution is unique): To guarantee the uniqueness, we assume that f is independent of one spatial variable: $f(x) = f(x_1)$. The observation on the boundary is assigned as follows

(a) On the whole boundary:

$$\psi(x) = \begin{cases} x_1 - 1, & x \in \Gamma_1, \\ \sin \pi x_2 + 2x_2^2, & x \in \Gamma_2, \\ x_1 + 1, & x \in \Gamma_3, \\ 2x_2^2 - 1, & x \in \Gamma_4. \end{cases}$$

(b) On a part of boundary (1) (observation is on x_1 axis):

$$\psi(x) = \begin{cases} x_1 - 1, & x \in \Gamma_1, \\ x_1 + 1, & x \in \Gamma_3, \end{cases}$$

or observation is on Γ_1 only:

$$\psi(x) = x_1 - 1, \quad x \in \Gamma_1.$$

(c) On a part of boundary (2): (observation is on x_2 axis)

$$\psi(x) = \begin{cases} \sin \pi x_2 + 2x_2^2, & x \in \Gamma_2 \\ 2x_2^2 - 1, & x \in \Gamma_4 \end{cases}$$

(d) or observation is on Γ_4 only

$$\psi(x) = x_1 - 1, \quad x \in \Gamma_4.$$

From the exact value of ψ we generate noise data as follows: first we discrete ψ which we denote by the same symbol, then we generates $\psi_\epsilon = \psi + \epsilon \,\mathrm{rand}(\cdot)$. Here $\mathrm{rand}(\cdot)$ is a random vector with L^2-norm equalling 1. The relative error of the data is defined by $\|\psi - \psi_\epsilon\|/\|\psi\|$, where $\|\cdot\|$ is the Euclidean norm of a vector (Table 1) .

We test these cases for the sought-for term $f(x) = f(x_1)$ of different smoothness:

Case 1: $f(x)$ is a very smooth function

$$f(x) = f_1(x_1) = (x_1^2 - 1)\sin \pi x_1$$

and $g(x) = g_1(x) = Lu - f_1(x_1)$.

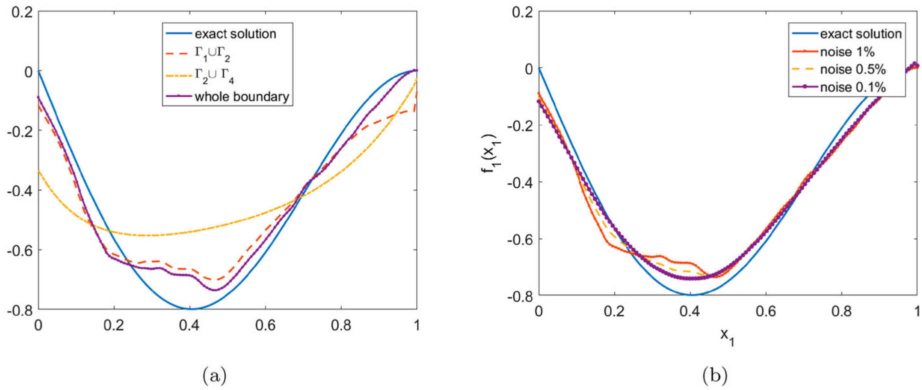

Figure 1. Example 4.1: Reconstruction of the smooth source function $f_1(x_1)$.

Case 2: $f(x)$ is a continuous but non-smooth function

$$f(x) = f_2(x_1) = \begin{cases} 2x_1, & x_1 \in \left(0, \dfrac{1}{2}\right] \times (0,1), \\ 1 - 2x_1, & x_1 \in \left(\dfrac{1}{2}, 1\right) \times (0,1) \end{cases}$$

and $g(x) = g_2(x) = Lu - f_2(x_1)$.

Case 3: $f(x) = f_3(x_1)$ is a discontinuous function

$$f(x) = f_3(x_1) = \begin{cases} 0, & x_1 \in (0, 0.3] \times (0,1) \cup [0.7, 1) \times (0,1), \\ 1, & x_1 \in (0.3, 0.7) \times (0,1) \end{cases}$$

and $g(x) = g_3(x) = Lu - f_3(x)$. In all of three above examples, the initial guess f^* is the mean value of $f(x)$ in Ω:

$$f^*(x) = \frac{1}{|\Omega|} \int_\Omega f(x)\,\mathrm{d}x.$$

Figure 1(a) shows the reconstructed source term for different observations, on $\Gamma_1 \cup \Gamma_2$, $\Gamma_2 \cup \Gamma_4$ and $\partial\Omega$, in comparison with the exact one. The noise level is 1% and the regularization parameter is 10^{-5}. Figure 1(b) depicts the numerical results for the observation on the whole boundary but with different noise levels, 0.1%, 0.5% and 1%. The regularization parameter is chosen to be 10^{-5}, 10^{-6} or 10^{-7}, respectively. From these figures we see that the observation in the whole boundary gives the best reconstruction. The worst case is when the observation is on Γ_2 or Γ_4 or on $\Gamma_2 \cup \Gamma_4$. The reason is that we have to find the function f depending on x_1 but the observation is a function of the variable x_2. It is also clear that if the noise level is small, the error in the reconstruction is also small. The numerical error of the tests is presented in Tables 2 and 3.

Table 2. Example 4.1: L_2-error in the non-smooth but continuous case with $\alpha = 10^{-5}$.

Noise(%)	0.1	0.5	0.1	0.5
Observation	$\Gamma_1 \cup \Gamma_2$	$\Gamma_1 \cup \Gamma_2$	Γ	Γ
L_2-error	0.04117	0.110359	0.0024	0.0092

Table 3. Example 4.1: L_2-error in the discontinuous case with different regularization parameters.

Noise(%)	0.001	0.001	0.01	0.01
Regularization parameter	10^{-7}	10^{-6}	10^{-7}	10^{-5}
L_2-error	0.114505	0.157848	0.180393	0.221967

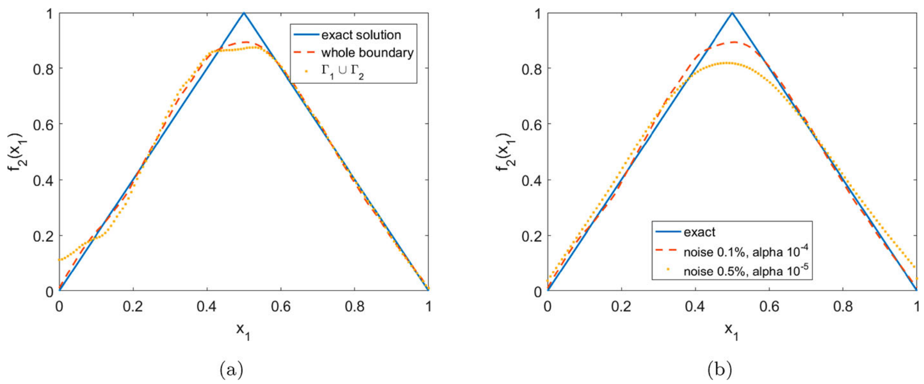

Figure 2. Example 4.1: Reconstruction of the continuous and non-smooth source function $f_2(x_1)$.

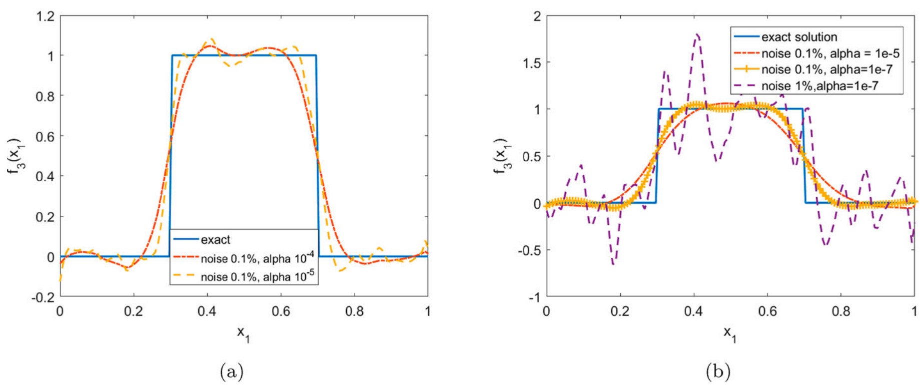

Figure 3. Example 4.1: Reconstruction of the discontinuous source function $f_3(x_1)$.

In the next two figures we present the numerical results for cases 2 and 3. We see that, although the examples are harder, but numerical results are still pretty good (Figures 2 and 3) .

In this example we have taken the initial guess f^* of the sought-for source f by its average value. However, the choice of f^* does not affect much the numerical solutions. For example, in Example 4.1, case 1, taking $\alpha = 10^{-4}$ for the relative noise 1%, and $\alpha = 10^{-5}$ for the relative noise 0.1%, we see that the numerical

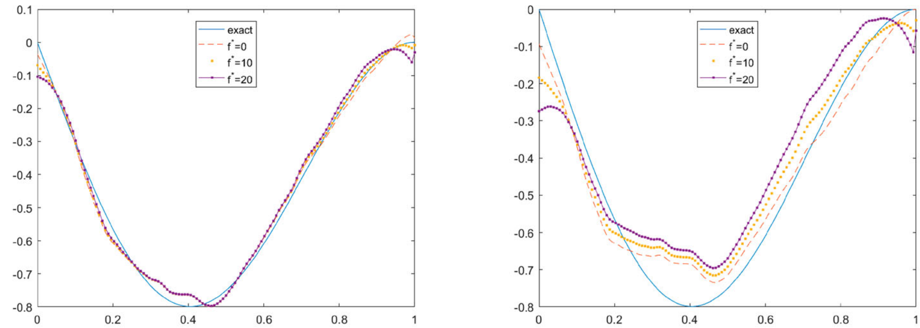

(a) Numerical results with relative noise 0.1% (b) Numerical results with relative noise 1%

Figure 4. Example 4.1, case 1: Exact and approximation solutions with $f^* = 0, 10$ and 20. (a) Numerical results with relative noise 0.1%; (b) Numerical results with relative noise 1%.

Table 4. Example 4.1, case 1: L^2 error between the exact solution and numerical ones with relative noise 0.1%, 1% for $f^* = 0, 10$, and 20.

f^*	0	10	20
L^2 error with relative noise 0.1%	0.020617	0.0198382	0.0239629
L^2 error with relative noise 1%	0.057949	0.071723	0.100642

results with $f^* = 0, 10$ and 20 presented in Figure 4 and Table 4 are not much different from each other. However, the choice of f^* is very important for the case of many solutions as the next example shows.

Example 4.2 (The solution is not unique): In general, if $f(x_1, x_2)$ depends on both variables x_1 and x_2, the solution is not unique. As described above, (u^0, f^0) is a solution to our inverse (1)–(2) with

$$\begin{cases} u^0 = x_1 \sin \pi x_2 + x_1 + 2x_2^2 - 1, \\ f^0 = (x_1^2 + 1) \sin \pi x_2 \end{cases}$$

with the observation of u being taken on the whole boundary of Ω as in Example 4.1. From Section 2.3, for any function $T(x_1, x_2) \in H^1(\Omega)$, the pair (u^T, f^T), defined by

$$u^T = u^0 + \xi^T, \quad f^T = f^0 + \frac{L\xi^T}{\hbar}, \quad \xi^T = T(x_1, x_2)x_1^2(x_1 - 1)^2 x_2^2 (x_2 - 1)^2, \tag{71}$$

is also a solution to the same inverse source problem. In this case, as the number of solutions is infinite, the prediction f^* to the sought-for term f plays an important role for selecting the solution. It has been proved in Theorem 2.5 that, if the regularization parameter is properly chosen, then the regularized solution $f_{\alpha h}^{\epsilon}$ converges to the unique f^*-solution of the inverse problem. It is difficult to represent the f^*-minimum norm solution in an explicit form, we therefore do some numerical tests for simulating it (Table 5) .

Table 5. Example 4.2: L_2-errors with f^* close to exact solutions.

Exact solution	$f^{20x_1+x_2}$	f^0	$f^{-5\sin\pi x_2}$	f^{-100x_1}
L_2-error	0.200252	0.050917	0.068730	0.740671

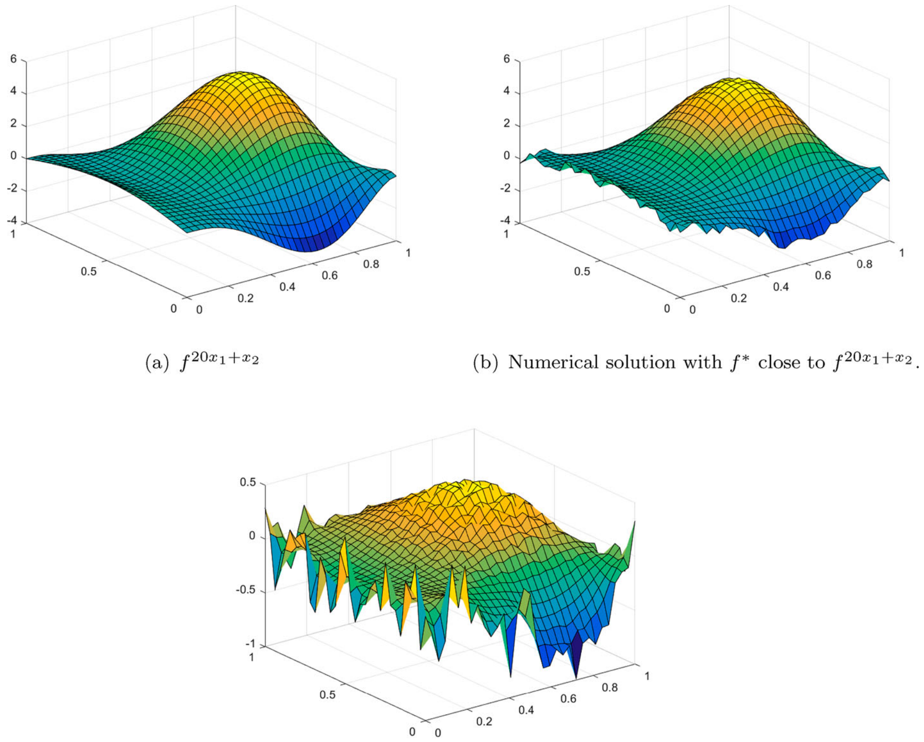

(a) $f^{20x_1+x_2}$

(b) Numerical solution with f^* close to $f^{20x_1+x_2}$.

(c) Error between $f^{20x_1+x_2}$ and the numerical solution with f^* close to $f^{20x_1+x_2}$.

Figure 5. Example 4.2: $f^{20x_1+x_2}$ and its numerical solution after 35 iterations with f^* close to $f^{20x_1+x_2}$. (a) $f^{20x_1+x_2}$]; (b) Numerical solution with f^* close to $f^{20x_1+x_2}$; (c) Error between $f^{20x_1+x_2}$ and the numerical solution with f^* close to $f^{20x_1+x_2}$.

We test for $T = 0$, $T = 20x_1 + x_2$ and $T = -5\sin\pi x_2$. We choose $\alpha = 10^{-5}$, and noise level of 1%. By varying f^* being near f^0, $f^{20x_1+x_2}$ and $f^{-5sin\pi x_2}$, we see that our algorithm can reconstruct the corresponding f^*-minimum norm solution, but the others. Indeed, first we choose $f^* = (0.9 + 0.01 * \text{rand}\,(-1,1))f^{20x_1+x_2}$, then after 35 iterations the L^2-norm error between $f^{20x_1+x_2}$ and its numerical solution reduces from 1.77696 to 0.200263 (Figure 5(c)). Thus, the numerical solution in this case approximates well $f^{20x_1+x_2}$, but f^0 and $f^{-5\sin\pi x_2}$, see Figure 5.

Similarly, if we choose f^* by $(0.9 + 0.01 * \text{ rand }(-1,1))f^0$ or $(0.9 + 0.01 * \text{rand }(-1,1))f^{-5\sin\pi x_2}$, then numerical solutions approximate well f^0 and $f^{-5\sin\pi x_2}$, respectively (see Figures 6 and 7). In these tests we see that the a priori

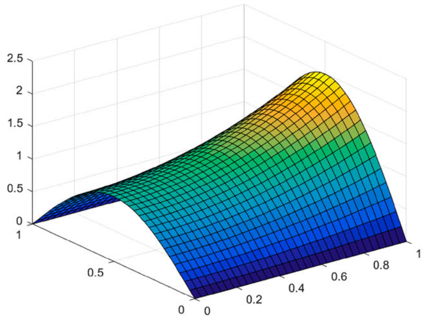

(a) f^0

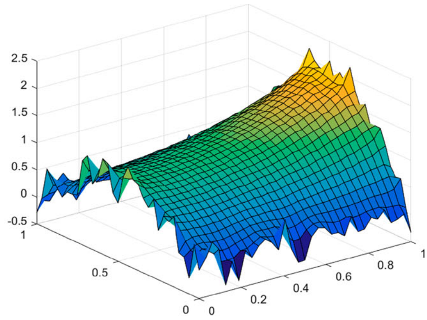

(b) Numerical solution with f^* close to f^0.

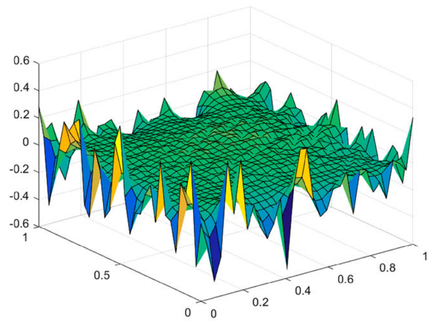

(c) Error between the numerical solution and f^0 with f^* close to f^0.

Figure 6. Example 4.2: f^0 and the numerical solution with f^* close to f^0. (a) f^0; (b) Numerical solution with f^* close to f^0; (c) Error between the numerical solution and f^0 with f^* close to f^0.

information is crucial for selecting the solution in the case of many solutions to the inverse source problem.

As we noted above, it is difficult to provide explicit examples for the inverse problem (1)–(2) where f satisfies the source condition (22). For illustrating theoretical results of Theorem 2.5, we construct such examples numerically as follows.

Example 4.3 (The source condition (22) for $\theta = 1/2$): We have to find an f of the form $f = f^* + A^*\Phi$, where $f^* \in L^2(\Omega)$ is an a priori information on f and Φ is an arbitrary function in $L^2(\Gamma)$. For this purpose we proceed as follows.

(1) Solve the problem

$$\begin{cases} Lp & = 0 \text{in } \Omega, \\ \dfrac{\partial p}{\partial \nu} + \sigma p & = \begin{cases} \Phi & \text{on } \Gamma, \\ 0 & \text{on } \partial\Omega \setminus \Gamma, \end{cases} \end{cases} . \tag{72}$$

From the definition of A in (8), we see that $A^*\Psi = \hbar p$.

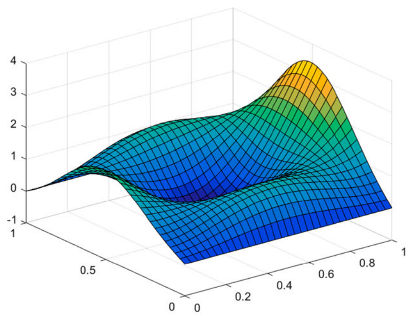

(a) $f^{-\sin(\pi x_2)}$

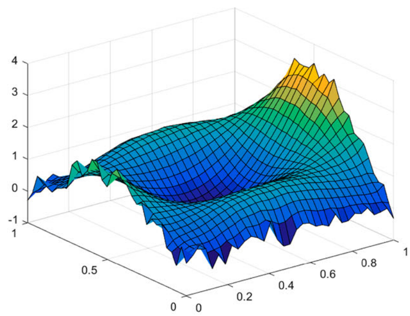

(b) Numerical solution with f^* close to $f^{-5\sin(\pi x_2)}$.

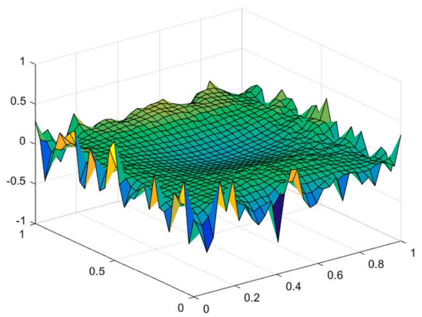

(c) Error between the numerical solution and $f^{-5\sin \pi x_2}$ with f^* close to $f^{-5\sin \pi x_2}$.

Figure 7. Example 4.2: $f^{-5\sin \pi x_2}$ and the numerical solution with f^* close to $f^{-5\sin \pi x_2}$. (a) $f^{-\sin(\pi x_2)}$; (b) Numerical solution with f^* close to $f^{-5\sin(\pi x_2)}$; (c) Error between the numerical solution and $f^{-5\sin \pi x_2}$ with f^* close to $f^{-5\sin \pi x_2}$.

(2) For the chosen f^*, from Lemma 3.1 we see that $f = f^* + A^*\Phi = f^* + \hbar p$ satisfies the source condition (22) for $\theta = 1/2$.

(3) Solve the problem

$$\begin{cases} Lu = f^* + \hbar p & \text{in } \Omega, \\ \dfrac{\partial u}{\partial \nu} + \sigma u = 0 & \text{on } \partial\Omega, \end{cases} \tag{73}$$

and set $\psi := u|_\Gamma$.

To test our algorithm due Theorem 2.5 we add some random noise with noise level ϵ to ψ to get the data ψ^ϵ (see the description in Example 4.1) and then choose

$$\alpha = \mathcal{O}(\epsilon^{\frac{3}{2}} + h^{\frac{1}{2}}),$$

where h is the mesh size of the FEM in (65).

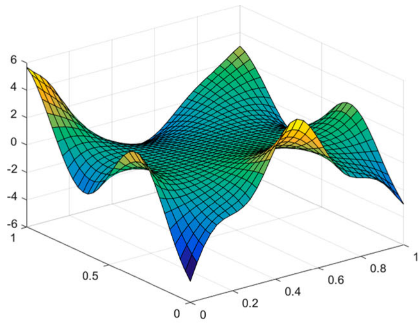

(a) Exact solution

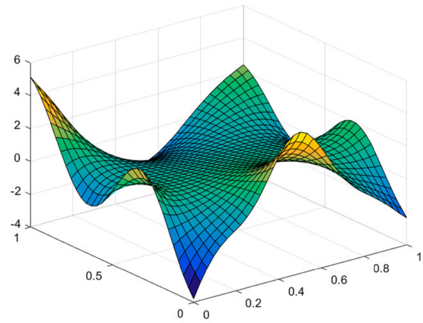

(b) Numerical solution

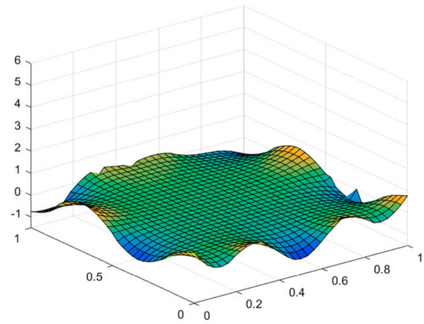

(c) Error between the exact and the numerical solution

Figure 8. Example 3: Numerical results for f satisfying the source condition (22) with $\theta = 1/2$. Relative noise $= 0.01\%$. (a) Exact solution; (b) Numerical solution; (c) Error between the exact and the numerical solution.

Table 6. Example 3: L^2-error behaviour.

Relative noise(%)	0.001	0.005	0.01
number of elements on the boundary/number of interior elements in the whole domain	632/99856	384/36864	224/12544
ϵ	0.000227827	0.00113913	0.00227827
h	0.00185375	0.00305097	0.00523024
α	4.55655e–05	2.27827e–04	4.55649-04
L^2-error	0.0369446	0.235932	0.391248

For numerical tests, we take $\hbar = 1, f^* = 0$, and $\Gamma = \partial\Omega$,

$$\Phi = 3\sin(5\pi x_1)(8\cos(\pi x_1 x_2) + 3) - 5\cos 2\pi x_1 \cos(3\pi x_2(x_2 + 9)).$$

We take $h^{\frac{4}{3}} = \mathcal{O}(\epsilon)$ and thus $\alpha = \mathcal{O}(\epsilon)$. From Theorem 2.5, the L^2-error of the method is of $\mathcal{O}(\epsilon^{\frac{1}{2}})$. This theoretical result is confirmed by the performance of the algorithm is presented in Figure 8 and Table 6.

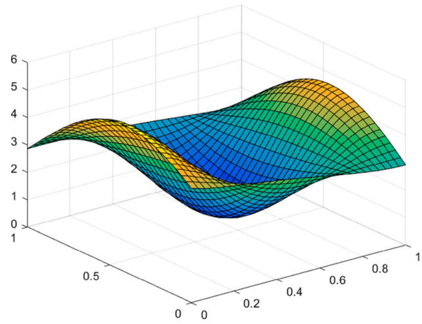

(a) Exact solution

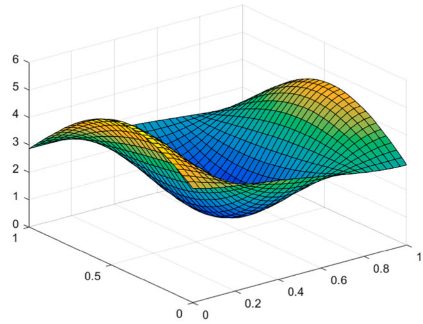

(b) Numerical solution

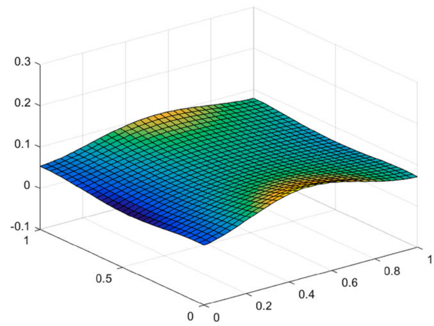

(c) Error between the exact and the numerical solution

Figure 9. Example 4: Numerical results for f satisfying the source condition (22) with $\theta = 1$. Relative noise $= 0.01\%$.(a) Exact solution; (b) Numerical solution; (c) Error between the exact and the numerical solution.

Example 4.4 (The source condition (22) for $\theta = 1$): We have to find an f of the form $f = f^* + A^*A\phi$, where $f^* \in L^2(\Omega)$ is an a priori information on f and ϕ is an arbitrary function in $L^2(\Omega)$. As in the previous example, we proceed as follows:

(1) Solve the problem

$$\begin{cases} Lv = \phi & \text{in } \Omega, \\ \dfrac{\partial v}{\partial \nu} + \sigma v = 0 & \text{on } \partial\Omega. \end{cases} \tag{74}$$

From the definition of A in (8), we see that $A\phi = v|_\Gamma$.

(2) Solve the problem

$$\begin{cases} Lp & = 0 \text{ in } \Omega, \\ \dfrac{\partial p}{\partial \nu} + \sigma p & = \begin{cases} v|_\Gamma & \text{on } \Gamma, \\ 0 & \text{on } \partial\Omega \setminus \Gamma, \end{cases} \end{cases} . \tag{75}$$

Table 7. Example 4: L^2-error behaviour.

Relative noise(%)	0.01	0.05	0.1
number of elements on the boundary/number of interior elements in the whole domain	320 / 25600	120 / 3600	72 / 1296
ϵ	0.000227826	0.00113914	0.00227795
h	0.00366116	0.00976311	0.0162718
α	0.00111907	0.00327208	0.00519378
L^2-error	0.00565496	0.0408677	0.0938595

From Lemma 3.1 we have that $A^*v|_\Gamma = A^*A\phi = \hbar p$.

(3) For the chosen f^*, we see that $f = f^* + \hbar p$ satisfies the source condition (22) for $\theta = 1$.

(4) Solve the problem

$$\begin{cases} Lu = f^* + \hbar p & \text{in } \Omega, \\ \dfrac{\partial u}{\partial \nu} + \sigma u = 0 & \text{on } \partial\Omega, \end{cases} \tag{76}$$

and set $\psi := u|_\Gamma$.

With ψ in hand, we then proceed as in Example 3. In this example, we take $\hbar = 1, f^* = 0$, and $\Gamma = \partial\Omega$,

$$\phi(x) = 8(4 + x_1)(\cos(2\pi x_1) + 3) + 3(4 + x_2)(\cos 2\pi x_2 + 3)$$

and

$$f^* = 2\sin(\pi x)\cos(2\pi y).$$

We take $h = \mathcal{O}(\epsilon^{\frac{2}{3}})$ and thus $\alpha = \mathcal{O}(\epsilon^{\frac{2}{3}})$. From Theorem 2.5, the L^2-error is $\mathcal{O}(\epsilon^{\frac{2}{3}})$. This theoretical result is confirmed by the performance of the algorithm is presented in Figure 9 and Table 7.

Disclosure statement

No potential conflict of interest was reported by the author(s).

Funding

This research is partially supported by Vietnam Institute for Advanced Study in Mathematics (VIASM), and the International Center for Research and Postgraduate Training in Mathematics, Institute of Mathematics, VAST under the grant ICRTM02-2020.03 (Dinh Nho Hào and Le Thi Thu Giang).

References

[1] Amirov AK.. On a problem on the solvability of inverse problems. Sibirsk Mat Zh. 1987;28(6):3–11. Sib Math J 1987;28:865–872.

[2] Isakov V. Inverse source problems. Providence (RI): American Mathematical Society; 1990.
[3] Khaidarov A. On estimates for and the existence of solutions of a class of inverse problems for elliptic equations. Dokl Akad Nauk SSSR. 1987;294(1):41–43.(Russian).
[4] Lavrent'ev MM, Romanov VG, Shishatskii GP. Ill-posed problems in mathematical physics and analysis. Providence (RI): American Mathematical Society; 1986.
[5] Prilepko AI. Inverse problems of potential theory (elliptic, parabolic, hyperbolic equation and transport equations). Mat Zametki. 1973;14:755–767. (Russian).
[6] Prilepko AI, Orlovsky DG, Vasin IA. Methods for solving inverse problems in mathematical physics. New York: Marcel Dekker Inc.; 2000.
[7] Vabishchevich PN. Uniqueness of the solution of an inverse problem for determining the right-hand side of an elliptic equation. Differ Uravn. 1982;18(8):1450–1453.(Russian).
[8] Amirov AK.. Solvability of inverse problems for a second-order equation. Funktsional Anal I Prilozhen. 1986;20(3):80–81. Engl transl. Funct Anal Appl 1986;20(3):236–237.
[9] Isakov V. Inverse problems for partial differential equations. Berlin: Springer-Verlag; 2006.
[10] Klibanov MV. Carleman estimates for global uniqueness, stability and numerical methods for coefficient inverse problems. J Inverse Ill-Posed Probl. 2013;21(4):477–560.
[11] Klibanov MV, Li JZ. Inverse problems and carleman estimates – global uniqueness, global convergence and experimental data. Berlin: De Gruyter; 2021.
[12] Khaidarov A. A class of inverse problems for elliptic equations. Differ Uravn. 1987;23(8):1376–1383.(Russian).
[13] Khaidarov A. A class of inverse problems for elliptic equations. Sibirsk Mat Zh. 1990;31(4):149–159. (Russian). Engl. Transl. Sib Math J 1990;31(4):657–666.
[14] Prilepko AI, Kostin AB, Solov'ev VV. Inverse problems on finding the source and coefficients for elliptic and parabolic equations in Hölder and Sobolev spaces. Sib Zh Chist Prikl Mat. 2017;17(3):67–85. (Russian). translation in J Math Sci (N.Y.) 2019;237(4):576–594.
[15] Vabishchevich PN. Uniqueness of some inverse problems for elliptic equations. Differ Uravn. 1988;24(12):2125–2129, 2206. (Russian). translation in Differ Equ 1988;24(12):1443–1446.
[16] Vabishchevich PN. Reconstruction of the right-hand side of the elliptical equation from observation data obtained at the boundary. Kragujev J Math. 2007;30:45–58.
[17] Yu WH. Well-posedness of determining the source term of an elliptic equation. Bull Aust Math Soc. 1994;50(3):383–398.
[18] Farcas A, Elliott L, Ingham DB, et al. A dual reciprocity boundary element method for the regularized numerical solution of the inverse source problem associated to the Poisson equation. Inverse Probl Sci Eng. 2003;11:123–139.
[19] Hinze M. A variational discretization concept in control constrained optimization: the linear-quadratic case. Comput Optim Appl. 2005;30(1):45–61.
[20] Tröltzsch F. Optimal control of partial differential equations: theory, methods and applications. Providence: American Mathematical Society; 2010.
[21] Budak BM, Samarskii AA, Tikhonov AN. A collection of problems in mathematical physics. Oxford: Pergamon Press; 1964.
[22] Kirsch A. An introduction to the mathematical theory of inverse problems. 3rd ed., Cham: Springer; 2021.
[23] Johnson C. Numerical solution of partial differential equations by the finite element method. Cambridge: Cambridge University Press; 1987.
[24] Grisvard P. Elliptic problems in nonsmooth domains. Boston (MA): Pitman; 1985.